THE JOURNAL OF PHYSICAL CHEMISTRY B

Article

pubs.acs.org/JPCB

Solvation and Proton-Coupled Electron Transfer Reduction Potential of $^2NO^•$ to ^1HNO in Aqueous Solution: A Theoretical Investigation

Mateus F. Venâncio,[†] Fabio Doctorovich,*[,‡] and Willian R. Rocha*[,†]

[†]Laboratório de Química Computacional e Modelagem Molecular (LQC-MM), Departamento de Química, ICEx, Universidade Federal de Minas Gerais, 31270-901, Pampulha, Belo Horizonte, MG, Brazil

[‡]Departamento de Química Inorganica, Analítica y Química Física, Facultad de Ciencias Exactas y Naturales (INQUIMAE-CONICET), Universidad de Buenos Aires, Ciudad Universitaria, Buenos Aires, Argentina

Supporting Information

ABSTRACT: In this work, quantum mechanical calculations and Monte Carlo statistical mechanical simulations were carried out to investigate the solvation properties of HNO in aqueous solution and to evaluate the proton-coupled one electron reduction potential of ^2NO to ^1HNO, which is essential missing information to understand the fate of ^2NO in the biological medium. Our results showed that the ^1HNO molecule acts mainly as a hydrogen bond donor in aqueous solution with an average energy of −5.5 ± 1.3 kcal/mol. The solvation free energy of ^1HNO in aqueous solution, computed using three approaches based on the linear response theory, revealed that the current prediction of the hydration free energy of HNO is, at least, 2 times underestimated. We proposed two pathways for the production of HNO through reduction of NO. The first pathway is the direct reduction of NO through proton-coupled electron transfer to produce HNO, and the second path is the reduction of the radical anion $HONO^{•-}$, which is involved in equilibrium with NO in aqueous solution. We have shown that both pathways are viable processes under physiological conditions, having reduction potentials of $E^{\circ\prime} = -0.161$ V and $E^{\circ\prime} \approx 1$ V for the first and second pathways, respectively. The results shows that both processes can be promoted by well-known biological reductants such as NADH, ascorbate, vitamin E (tocopherol), cysteine, and glutathione, for which the reduction potential at physiological pH is around −0.3 to −0.5 V. The computed reduction potential of NO through the radical anion $HONO^{•-}$ can also explain the recent experimental findings on the formation of HNO through the reduction of NO, promoted by H_2S, vitamin C, and aromatic alcohols. Therefore, these results contribute to shed some light into the question of whether and how HNO is produced in vivo and also for the understanding of the biochemical and physiological effects of NO.

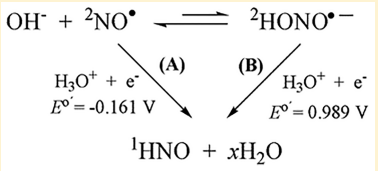

INTRODUCTION

Nitric oxide ($NO^•$) is an important signaling molecule and plays a key role in a wide variety of biochemical and physiological processes in the human body as, for instance, modulation of the immune and endocrine response, cardiovascular control, regulation of blood pressure, neurotransmission, induction of apoptosis, among others.[1−10] The discovery that NO is involved in controlling the vascular tone, as the elusive endothelial-derived relaxing factor (EDRF),[1] has stimulated much research on the biochemical functions and possible therapeutic applications[5−10] of NO, and in 1992, NO was named "Molecule of the Year" by Science.[11]

Historically, $NO^•$ reduction to HNO/NO^- in aqueous solutions has been considered to not be relevant in biological media, taking into account that the reduction potential of $NO^•$ is quite negative and outside of the biologically compatible range ($E^\circ(NO^•/NO^-) = -0.81$ V vs NHE).[12,13] At physiological pH, this process renders the protonated species ^1HNO, and as estimated by Lymar and co-workers,[12] it has a less negative redox potential, being $E^\circ(NO^•, H^+/HNO) = -0.14$ V vs NHE and $E^{\circ\prime} = -0.55$ V (pH 7).[12] However, it should be mentioned that biological reducing agents such as NADH and cysteine have reduction potentials around −0.3 V. Therefore, one electron reduction of $NO^•$ to HNO at pH ca. 7 is still not a biologically favorable process when the estimated value of −0.14 V is taken as a reference. Moreover, it has been recently shown that NO can be reduced to ^1HNO by ascorbate (vitamin C) and aromatic alcohols,[14,15] i.e., those alcohols that have a tendency toward the formation of more stable free radicals $RO^•$ by oxidation. In all cases, the redox potential is unfavorable for NO reduction ($E^{\circ\prime}(RO^•, H^+/ROH)$) at pH 7 ranges from +0.10 to +0.97 V for these alcohols. At this point, it is relevant to mention that $E^\circ(NO^•, H^+/HNO)$ cannot be measured directly due to the irreversibility of the $NO^•/HNO$ redox couple. The assessment reported by Lymar[12] was done assuming $\Delta G_f^\circ(HNO(aq) \sim 115$ kJ/mol.[2] However, if this number is overestimated, the $NO^•/HNO$ redox couple could be inside the thermodynamic range of many biological reductants. As an example, if $E^\circ(NO^•, H^+/HNO)$ were shifted 0.3 V (i.e., E° ca. +0.16 V), then $E^{\circ\prime}$ would be −0.25 V at pH 7, a redox value compatible with NADH and cysteine oxidation. In fact, as we shall see later, the estimated solvation free energy of ^1HNO (between −1.7 and −5.0 kJ/mol) made by Lymar and Shafirovich is indeed underestimated, and this under-

Received: April 14, 2017
Revised: June 11, 2017
Published: June 16, 2017

DOI: 10.1021/acs.jpcb.7b03552
J. Phys. Chem. B 2017, 121, 6618−6625

estimation has an important impact in the calculation of the NO•/HNO reduction potential.

Computational chemistry calculations have assisted the understanding of several structural, spectroscopic, and mechanistic properties related to the chemistry and biochemistry of HNO and NO.[16] However, despite the size of the system, the proton-coupled electron transfer reduction of NO to ^{1}HNO in aqueous solution, as far as we know, has not yet been addressed by these calculations. The theoretical treatment of the NO/^{1}HNO reduction potential in aqueous solution is also a challenging process for computational studies, requiring the correct description of the solvent media, representation of the proton in solution, and also an adequate electronic structure method to treat these species in different electronic states. We believe that the correct estimation of the NO•/HNO reduction potential is essential to shed some light onto the question of whether and how HNO is produced in vivo, contributing to the understanding of the biochemical and physiological effects of NO.

In this context, in this work, we have combined Monte Carlo statistical mechanics simulations and quantum mechanical calculations to investigate the solvation of HNO and the proton-coupled electron transfer reduction potential of NO•/HNO. As we shall see, the solvation free energy of HNO is at least 2 times more favorable than the actual estimated value, and the NO•/HNO reduction potential can be as much as +1 V at physiological pH, meaning that NO can indeed be reduced to HNO in biological media.

THEORETICAL DETAILS

Equilibrium geometries and numerical frequencies for the NO and HNO molecules were obtained at the density functional theory[17] level, using the TPSSh exchange-correlation functional,[18] second order Møller−Plesset perturbation theory,[19] and coupled-cluster theory with single, double, and interactive triple excitations, CCSD(T).[19−21] For both methods, the def2-TZVP, def2-TZVPP, def2-QZVP, and def2-QZVPP basis sets[22] were employed. Gas phase Gibbs free energy contribution to the reduction potential was obtained directly from the numerical frequency calculations. The solvation free energy contributions were obtained from single-point calculations, at the optimized geometries, using the SMD model of Truhlar and Cramer,[23] with the electrostatic contribution to the solvation free energy obtained using the conductor-like screening model (COSMO) of Klamt,[24] hereafter called the COSMO/SMD approach.

In order to better understand the behavior of HNO in aqueous solution, Monte Carlo (MC) statistical mechanical simulations[25] were carried out in the NpT ensemble at 298 K and 1 atm. The simulations were composed of one solute molecule (the HNO molecule) and 800 water molecules in a cubic box of 28.866 Å per side, applying the periodic boundary conditions and minimum image convention.[25] The system was equilibrated with 40,000 MC steps, followed by an additional averaging stage of 60,000 MC steps to obtain the thermodynamic properties. A new configuration is generated after all solvent molecules sequentially attempt to translate in all Cartesian directions and also attempt to rotate around a randomly chosen axis. Therefore, the total number of configurations generated by the MC simulation was 48×10^6. The energy at each MC step was evaluated using a classical intermolecular pair potential composed of the 12−6 Lennard-Jones (LJ) plus Coulomb terms.[25] The water molecules were described with the TIP3P model[26] and the solute molecule by the OPLS force field,[27] with the atomic charges obtained through the CHELPG method.[28]

To reduce the number of supermolecular clusters submitted for quantum mechanical calculations (vide infra), the configurations were selected according to the autocorrelation function of the energy.[29,30] From this a total of 150 uncorrelated configurations were selected, with less than 5% of statistical correlation, and used in the quantum mechanical calculation. All Monte Carlo simulations were performed using the DICE program developed by Canuto and Coutinho.[31]

The solvation free energy of ^{1}HNO was computed using three different approaches. The first approach comes from the linear response theory (LRT)[32,34] and is shown in eq 1:

$$\Delta G_{solv} = \frac{1}{2}\langle \Delta U_{short} \rangle + \langle E_{diel}^{cluster} - E_{diel}^{solvent} \rangle \quad (1)$$

This approach, proposed by Pliego Jr. and co-workers,[34] has been used to obtain solvation free energies of ions in aqueous solution. The first term on the right describes the average value of the energies involved in the solute−solvent short-range interactions (hydrogen bonds in the present case). This term was obtained through single point energy calculations at the TPSSh/Def2-QZVP level of theory on every hydrogen bonded uncorrelated configuration obtained from the Monte Carlo simulation. The second term of eq 1 describes the solute−solvent long-range dielectric interaction. It is divided into two terms: (i) the dielectric interaction between the hydrogen bonded cluster with the dielectric, $E_{diel}^{cluster}$, and (ii) the dielectric interaction of only the solvent molecules (in their geometries of the cluster) composing the cluster, $E_{diel}^{solvent}$. The dielectric interactions were obtained through single point calculations using the COSMO model.[23] In the 150 uncorrelated configurations analyzed, only 101 configurations show hydrogen bonds; therefore, the computation of the first term of eq 1 involved 202 single point energy calculations at the TPSSh/Def2-QZVP level of theory. For the computation of the second term of eq 1, an additional 202 single point energy calculations at the TPSSh/Def2-QZVP/COSMO level were performed. Therefore, the computation of the solvation free energy following eq 1 involved a total of 404 single point energy calculations.

The second approach used to obtain the solvation free energy of ^{1}HNO was to employ the expression derived from the LRT, proposed by Carlson and Jorgensen,[33]

$$\Delta G_{solv} = \alpha\langle U_{vdW} + U_{ele} \rangle + \gamma(\mathrm{SASA}) \quad (2)$$

where the constants α = 0.310 and γ = 0.014 kcal·mol^{-1}·Å^{-2} were obtained by Carlson and Jorgensen[33] though a linear fitting procedure to reproduce the experimental free energy of hydration of 13 organic molecules of different sizes and functions. Using Monte Carlo simulations with the OPLS force field,[27] the fitting procedure generated an rms deviation of 0.88 kcal/mol compared with the experimental values. The first term on the right side of eq 2 is the average solute−solvent interaction energy obtained straight from the Monte Carlo simulation (energies from the Coulomb + LJ intermolecular interaction potential), and the second term is the contribution from the cavitation energy being proportional to the solvent accessible surface area (SASA) of the solute. The advantage of using this approach is that the necessary data comes straight from the Monte Carlo simulation and there is no need for additional quantum mechanical calculations. The third

DOI: 10.1021/acs.jpcb.7b03552
J. Phys. Chem. B 2017, 121, 6618−6625

approach used to compute the ΔG_{solv} of ^{1}NHO was employing the SMD/COSMO approach at the TPSSh/Def2-QZVP level of theory.

All quantum mechanical calculations reported in this work were performed with the ORCA program.[35]

RESULTS AND DISCUSSION

Solvation of HNO. The molecular structure of ^{1}HNO, used in the MC simulation, was optimized at the TPSSh/Def2-QZVP level and shows r_{NH} = 1.065 Å, r_{NO} = 1.201 Å, and ∠HNO = 108.64°. Figure 1 shows the radial pair distribution,

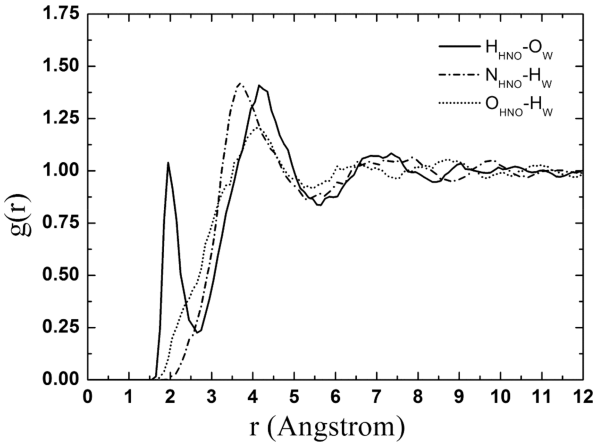

Figure 1. Radial pair distribution functions, $g(r)$, involving HNO and water. $H_{HNO}-O_W$ is the $g(r)$ between the hydrogen atom of HNO and the oxygen atoms of water. $N_{HNO}-H_W$ is the $g(r)$ between the nitrogen atom of HNO and the hydrogen atoms of water. $O_{HNO}-H_W$ is the $g(r)$ between the oxygen atom of NHO and the hydrogen atoms of water.

$g(r)$, between HNO and water. The $g(r)$ involving the hydrogen of HNO and the oxygen of water shows a sharp peak, starting at 1.6 Å and centered at 1.95 Å, typical from hydrogen bonding interactions. Integration of this $g(r)$ from 1.6 to 2.65 Å gives an average of 1.04 water molecules as nearest neighbors. On the other hand, the $g(r)$ involving the nitrogen and oxygen atoms of HNO with the hydrogen of water do not show hydrogen bonding peaks. The $g(r)$ between the nitrogen and the hydrogen of water shows a well-defined first peak centered at a long distance of 3.65 Å. This corresponds to the average distance that the hydrogen atom of water stays from the nitrogen of HNO in the first solvation shell, along the entire simulation. The first solvation shell of the oxygen atom of HNO shows the hydrogen atoms of the solvent at an even further average distance of 4.15 Å. These structural results show that the nitrogen and oxygen atoms of HNO are not involved in hydrogen bonds with the solvent.

Hydrogen bonds are also obtained using a geometric and energetic criterion. We consider a hydrogen bond formation when the distance is RDA ≤ 3.2 Å, the angle is ∠AHD ≤ 30°, and the interaction energy is lower than 0 kcal/mol. That is, all stabilizing interaction that satisfies the geometric criteria is considered as a hydrogen bond. The results of the hydrogen bond analysis are quoted in Table 1. From the 150 uncorrelated configurations, only in 101 configurations do we obtain hydrogen bonds, meaning that in only 67.3% of the configurations the HNO makes hydrogen bonds with the solvent. In these 101 configurations, 87 show only one

Table 1. Statistics of the Hydrogen Bonds (HBs) Formed between ^{1}HNO and Water[a]

HB site of HNO	occurrence (%)	energy (kcal/mol)	average distance (Å)
H	95 (79.8)	−5.5 ± 1.3	1.998 ± 0.121
N	3 (2.5)	−1.7 ± 0.4	2.268 ± 0.025
O	21 (17.7)	−1.9 ± 0.7	2.130 ± 0.121

[a]Statistics of the hydrogen bonds in the 101 configurations in which HNO makes HBs with the solvent.

hydrogen bond, corresponding to 86.1%, 12 configurations show two hydrogen bonds (11.9%), and only 2 configurations show three hydrogen bonds corresponding to only 2% of the configurations. Therefore, in the majority of the configurations, the HNO molecule makes only one hydrogen bond with the solvent. In these 101 configurations, we found a total of 119 hydrogen bonds. As can be seen in Table 1, the main hydrogen bond making site is the hydrogen atom of HNO for which we found 95 hydrogen bonds with the oxygen of the water molecules, corresponding to 79.8% of the hydrogen bonds. The oxygen atom appears as a hydrogen bond acceptor 21 times, corresponding to 17.7% of the hydrogen bonds, and hydrogen bonds involving the nitrogen atom as an acceptor appear only 3 times (2.5%). Representative examples of hydrogen bonded structures of HNO with one, two, and three solvent molecules, obtained from the 150 uncorrelated configurations from the MC simulations, are shown in Figure 2.

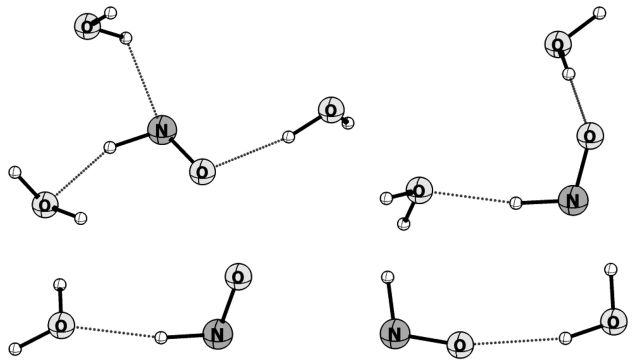

Figure 2. Representative examples of hydrogen bonded structures of HNO with one, two, and three solvent molecules, obtained from the statistically uncorrelated configurations from the Monte Carlo simulation.

The energies involved in the hydrogen bonds are also quoted in Table 1. The hydrogen atom of ^{1}HNO makes stronger hydrogen bonds with the solvent, with an average value of −5.5 ± 1.3 kcal/mol. The nitrogen and oxygen atoms of HNO make hydrogen bonds with average values of −1.7 ± 0.4 and −1.9 ± 0.7 kcal/mol, respectively.

The hydration free energy of HNO was computed using the linear response theory (LRT) approaches represented by eqs 1 and 2, and also using the SMD/COSMO solvation model, and the results are quoted in Table 2. As we can see, all methods produce much higher solvation free energies than the estimated value[12] (between −1.7 and −5.0 kJ/mol) on the basis of structural analogies with HCN and H_2CO. This difference can certainly be attributed to the hydrogen bonds formed when ^{1}HNO is solvated. The hydration free energy of −1.68 ± 0.78 kcal/mol calculated using eq 2, with the average solute−solvent

DOI: 10.1021/acs.jpcb.7b03552
J. Phys. Chem. B 2017, 121, 6618−6625

Table 2. Solvation Free Energy of ^{1}HNO Obtained by Different Approaches

approach[a]	ΔG_{solv} (kcal/mol)
$\Delta G_{solv}{}^1 = \frac{1}{2}\langle \Delta U_{short} \rangle + \langle E_{diel}^{cluster} - E_{diel}^{solvent} \rangle$	(−4.17 ± 0.95)
$\Delta G_{solv}{}^2 = \alpha \langle U_{vdW} + U_{ele} \rangle + \gamma(SASA)$	(−1.68 ± 0.78)[b]
$\Delta G_{solv}{}^3$ = COSMO/SMD	−4.62

[a]See the Theoretical Details section for a description of the methods used. [b]The solvent surface area (SASA) of HNO (152.60 Å^2) was computed using the molecular surface module of MarvinView package.[48] The average solute−solvent energy, $\langle U_{vdW} + U_{ele} \rangle$ = −12.30 ± 0.78 kcal/mol was obtained straight from the MC simulation.

interaction energy from Monte Carlo simulation, is more than 2 kcal/mol higher than −4.17 ± 0.95 kcal/mol, obtained using the more time-consuming approach from eq 1. It is worth noting that the result obtained with the SMD/COSMO protocol (−4.62 kcal/mol) is close to the results obtained with the sequential Monte Carlo/quantum mechanical treatment from eq 1. Unfortunately, the experimental hydration free energy of HNO is unknown. However, both methods used in this work show that the estimated solvation free energy of ^{1}HNO used to obtain the experimental reduction potential ^{2}NO/^{1}HNO is, at least, 2 times underestimated.

^{2}NO•/^{1}HNO Reduction Potential. The reduction potential of NO/HNO was computed using eq 3, as described by Rulíšek[36]

$$E^0\ [\mathrm{V}] = 27.21(G_{ox}\ [\mathrm{a.u.}] - G_{red}\ [\mathrm{a.u.}]) - E^0_{abs}(\mathrm{NHE})\ [\mathrm{V}] \quad (3)$$

where $G_{ox/red}$ is the Gibbs free energy of the oxidized/reduced forms and E^0_{abs}(NHE) is the absolute potential of the normal hydrogen electrode for which, in this work, we used the recommended value of 4.281 V suggested by Isse and Gennaro.[37] The Gibbs free energy of the species is obtained using eq 4

$$G = E_{elec-nuc} + \Delta G_{solv} + G_{term} \quad (4)$$

where ΔG_{solv} is the solvation free energy, G_{term} is the thermal contribution to the gas phase Gibbs free energy, obtained within the rigid rotor/harmonic oscillator approach, and $E_{elec-nuc}$ is the electronic−nuclear energy of the species. From eq 4, it can be seen that the solvation Gibbs free energy and the electronic energy are the main contributions for the computation of the reduction potential, since the thermal contributions are usually small and cancel out among the redox pair. The Gibbs free energy of solvation was obtained using, initially, the SMD/COSMO model. The approach used here has been used successfully to describe the reduction potential of transition metal compounds.[36,38]

In order to validate this approach, we first applied it to describe the reduction potential of similar NO species for which experimental data are available, as those shown in Table 3. The effect of basis set and electronic structure methods on the computed reduction potential was tested for the reduction of nitric oxide to the nitroxyl anion (^{2}NO/^{3}NO$^-$), which has a reduction potential of $E°$ = −0.8 ± 0.2 V vs NHE.[13] The reduction potential was computed using the structure and harmonic frequencies of ^{2}NO and ^{3}NO$^-$ obtained at the DFT, MP2, and CCSD(T) levels of theory, with different basis sets, as shown in Table 4. As can be seen, the TPSSh functional

Table 4. Computed (^{2}NO/^{3}NO$^-$) Reduction Potentials with Different Basis Sets and Theoretical Methods

	$E°(^2\mathrm{NO}/^3\mathrm{NO}^-)$ vs NHE [V]		
basis set	TPSSh	MP2	CCSD(T)
Def2-TZVP	−0.91	−1.13	−1.13
Def2-TZVPP	−0.91	−1.13	−1.23
Def2-QZVP	−0.83	−0.98	−1.06
Def2-QZVPP	−0.83	−0.98	−1.06

provides much better results than MP2 and CCSD(T). The TPSSh/Def2-QZVP value of −0.83 V is in very good agreement with the experimental value of −0.8 ± 0.2 V. The CCSD(T) results provide the larger deviation (0.25 V) from the experimental value. Therefore, it seems that the protocol to compute the reduction potential, applying the SMD solvation model to obtain the solvation free energies, works better employing DFT methods in the electronic structure part. The hybrid meta-GGA functional TPSSh provides good results, as was also obtained for transition metal compounds.[38]

We have recently shown[39] by *ab initio* molecular dynamics that ^{2}NO in aqueous solution is involved in a reversible equilibrium, starting around 700 fs, generating the radical anion species HONO$^{\bullet-}$, according to Scheme 1. This radical anion

Scheme 1

$$OH^-_{(aq.)} + {}^2NO^{\bullet}_{(aq.)} \rightleftharpoons {}^2HONO^{\bullet-}_{(aq.)}$$

species can trap one electron and, therefore, be involved in a competitive reduction process with ^{2}NO, as shown in Scheme 2, opening up a new pathway for the reduction of ^{2}NO to

Table 3. Computed and Experimental Reduction Potentials for Some NO Compounds vs NHE

reaction couple	$E_{pred}°$ [a] (V)	$E_{calc}°$ [b] (V), this work	$E_{exp}°$ [c] (V)
2NO + e$^-$/ONNO$^-$	−0.1 ± 0.3	−0.16	−0.38
HONNO + H_3O^+ + e$^-$/HONNOH + H_2O	1.6 ± 0.3	1.70	1.75
^{2}NO + e$^-$/^{3}NO$^-$	−0.9 ± 0.3	−0.83	−0.81
NO_2 + e$^-$/ NO_2^-	0.6 ± 0.3	0.69	
NO_3 + e$^-$/ NO_3^-	1.9 ± 0.3	2.11	
$^2NO_2$ + H^+ + e$^-$/$^1HNO_2$		1.34	1.09[d]
^{2}NO + H^+ + e$^-$/^{1}HNO		0.27	−0.14[e]

[a]Values computed by Dutton and co-workers[44] at the CBS-QB3 level of theory. [b]Values computed at the TPSSh/Def2-QZVP/COSMO(SMD) level, treating the proton as Zundel ion $[H_2O{-}H{-}OH_2]^+$. [c]References 43 and 47. [d]Obtained through the equilibrium constant of the $N_2O_{4(g)}$/$2NO_{2(g)}$ and the ΔG value for the $N_2O_{4(g)}$, $2H^+$, $2e^-$/$2HNO_{2(aq)}$ reaction. [e]Taken from ref 12.

DOI: 10.1021/acs.jpcb.7b03552
J. Phys. Chem. B 2017, 121, 6618−6625

Scheme 2

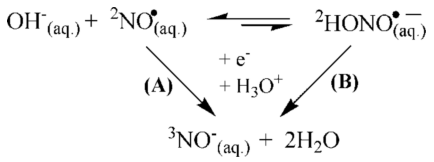

$^3NO^-$. The reduction potential for pathway B in Scheme 2 was also computed at the TPSSh/Def2-QZVP/SMD level, yielding a positive reduction potential of E^0 = 1.7 V. Therefore, these two competitive reduction pathways may be the source for the different, sometimes positive, experimental values reported for the reduction potential of ^2NO to $^3NO^-$, as was said previously.

The gas phase TPSSh/Def2-QZVP optimized structures, as well as Cartesian coordinates, used to compute the reduction potential of all species quoted in Table 3, can be found in the Supporting Information. In general, as can be seen in Table 3, our TPSSh/Def2-QZVP/SMD protocol provides good results for the reduction potential of NO_x species as compared with the experimental values and they are also in line with the values predicted by Dutton et al.,[44] with energetics obtained at the CBS-QB3 level of theory and solvation energies obtained through the C-PCM model. Since the reduction potential for the ^2NO, $H^+/^1HNO$ couple is not known experimentally, we used a similar process, $^2NO_2$, $H^+/^1HNO_2$, in which the reduction proceeds through a proton-coupled electron transfer (PCET) to the doublet reactant ($^2NO_2$) to generate the singlet product ($^1HNO_2$). For this process, the proton was treated as the conventional H_3O^+ and as the Zundel ion $[H_2O\cdots H\cdots OH_2]^+$.[45] The experimental value for this process (1.09 V vs NHE) was obtained through the equilibrium constant for the reaction $N_2O_4(g) \rightarrow 2NO_2(g)$ (0.137 ± 0.001 atm)[46] and the ΔG value for the reaction $N_2O_4(g) + 2H^+ + 2e^- \rightarrow 2HNO_2(aq)$ (−210.44 kJ/mol).[42] The TPSSh/Def2-QZVP/SMD computed reduction potential using the H_3O^+ cation is 1.78 V, which deviates 0.69 V from the experimental estimation. However, treating the proton as a Zundel cation improves the results reducing the computed value to 1.34 V with a much acceptable deviation of 0.25 V compared with the experiment. It is worth mentioning that the reduction potential for the radical anion shown in Scheme 2 also reduces to 1.420 V vs NHE, when the proton is treated as the Zundel cation. The reason for the better agreement between the computed reduction potentials with the experimental values can be attributed to the higher stability of the Zundel cation in water. These results show that the Zundel cation is more appropriate to calculate the PCET reduction potentials.

After validating our protocol, the reduction potential of $^2NO^\bullet$ to ^1HNO was then computed according to Scheme 3. As

Scheme 3

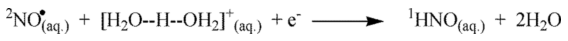

was emphasized in the Introduction, the determination of the reduction potential $E^\circ(^2NO, H^+/^1HNO)$ is of great importance due to the inherent difficulty associated with the instability of HNO in aqueous environment. Also, the accurate determination of this reduction potential may contribute enormously to the understanding of the genesis and reactivity of ^1HNO in the biological environment. As is shown in Table 3, the computed reduction potential $E^\circ(^2NO, H^+/^1HNO)$ at the TPSSh/Def2-QZVP/SMD level was 0.270 V vs NHE. It is worth noting that treating the cation as H_3O^+ the reduction potential obtained is 0.579 V, which is more than twice the value obtained with the Zundel ion. Our results, therefore, show that the reduction of $^2NO^\bullet$ to ^1HNO is a favorable process and, thus, very different from the reported value of −0.14 V obtained by Shafirovich and Lymar,[12] which was obtained using the experimental values for the enthalpy of formation[41] and standard entropy of HNO[42] and standard Gibbs free energy of formation of NO[40] and assuming that the hydration energy of HNO is in the same order of magnitude of HCN and H_2CO (approximately −5 and −1.7 kJ/mol, respectively). However, as we have shown in this work, the hydration free energy of ^1HNO is at least 2 times greater than the estimated value and, therefore, may have an important impact on the calculation of the reduction potential.

The theoretical results presented in this work, in conjunction with our previous ab initio molecular dynamics study,[39] give us support to propose the processes shown in Figure 3, which can

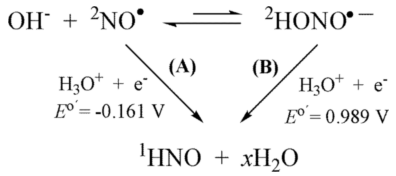

Figure 3. General scheme for the reduction of NO to HNO. x = 1 in pathway A, and x = 2 in pathway B.

be involved in the reduction of NO to HNO in aqueous solution. NO is involved in equilibrium with the radical anion $HONO^{\bullet-}$ which opens two possible pathways for the reduction of NO, as shown in Figure 3. According to our calculations, the direct reduction of NO by proton-coupled electron transfer in pathway A has a reduction potential of E° = 0.270 V vs NHE and $E^{\circ\prime}$ = −0.161 V at physiological pH (pH 7). HNO can also be formed through the reduction of the radical anion species, following pathway B, with a reduction potential of 1.420 V vs NHE and $E^{\circ\prime}$ = 0.989 V at pH 7. Our results show that the direct reduction of NO through pathway A is a viable process under physiological conditions, since $E^{\circ\prime}$ = −0.161 V is higher than the reduction potential around −0.3 V of well-known biological reductants such as NADH, vitamin C (ascorbate)[15] and vitamin E ($E^{\circ\prime}$ = −0.48 V),[14] cysteine, and glutathione. According to our calculations, the formation of HNO can be even more favorable through pathway B, with $E^{\circ\prime} \approx 1$ V. Interestingly enough, this new reduction potential can explain several redox processes involving the direct reduction of NO to HNO. For instance, Filipovic and co-workers have recently shown that HNO can be produced in vivo by the reaction of NO or nitrosyl species with H_2S.[49−52] This reaction would never happen considering the computed reduction potential $E^{\circ\prime}(NO, H^+/HNO)$ = −0.161 V (at pH 7), since $E^{\circ\prime}(S^{\bullet-}, 2H^+/H_2S) = E^{\circ\prime}(S^{\bullet-}, H^+/HS^-)$ = 0.92 V at pH 7.[51] The reduction potential computed for route B can explain this redox process, since $E^{\circ\prime} = (HONO^{\bullet-}, H^+/HNO)$ = 0.989 V at pH 7. In addition, Doctorovich and co-workers have recently shown that NO can be reduced to ^1HNO by vitamin C and aromatic alcohols.[14,15] However, in all cases, the redox potential is unfavorable for NO reduction ($E^{\circ\prime}(RO^\bullet, H^+/ROH)$) at pH 7 ranges from +0.10 to +0.97 V for these alcohols. These redox processes can also be explained by the reduction potential $E^{\circ\prime}$ =

DOI: 10.1021/acs.jpcb.7b03552
J. Phys. Chem. B 2017, 121, 6618−6625

($HONO^{\bullet-}$, H^+/HNO) = 0.989 V found in route B. Therefore, it seems that the radical anion $HONO^{\bullet-}$ may play an important role in the direct reduction of NO to HNO. It should be mentioned, however, that the route leading to the formation of this species is limited by the equilibrium constant involving NO and the radical anion $HONO^{\bullet-}$ which, according to our estimations, should be small. The experimental detection of this species is not an easy task; efforts in this regard are underway as well as the experimental investigation of the reaction of biological reductant agents with NO, and the results will be published in the near future.

It is worth mentioning that the reduction potentials computed here for pathways A and B are based on the computation of thermodynamical quantities, that is, the Gibbs free energy of reaction involved in the proton-coupled electron transfer reduction. However, the reactions involved in pathways A and B are spin forbidden and, therefore, the spin crossover of the intermediates along the proton-coupled electron transfer can also influence the reaction. The calculations reported here cannot take into account these nonadiabatic effects. Studies employing the non-adiabatic transition state theory (NA-TST)[53,54] to investigate these reactions are in progress.

CONCLUSIONS

In this work, quantum mechanical calculations and Monte Carlo statistical mechanical simulations were carried out to investigate the solvation properties of HNO in aqueous solution and to evaluate the reduction potential of ^{2}NO to ^{1}HNO, which are essential missing information to understand the fate of ^{2}NO in the biological medium.

Our results showed that the ^{1}HNO molecule acts mainly as a hydrogen bond donor in aqueous solution with an average energy of -5.5 ± 1.3 kcal/mol. The frequency of hydrogen bonds on the nitrogen and oxygen atoms acting as acceptors is small, with average energies of -1.7 ± 0.4 and -1.9 ± 0.7 kcal/mol, respectively. The solvation free energy of ^{1}HNO in aqueous solution was computed using three different approaches, two based on the linear response theory and the other based on the COSMO/SMD continuum approach. The solvation free energy was computed as -4.17 ± 0.95 and -1.68 ± 0.78 kcal/mol for the two approaches based on LRT and -4.62 kcal/mol using the COSMO/SMD approach. These results revealed that the hydration free energy of ^{1}HNO is at least 2 times greater than the value of -5 kJ/mol estimated previously on the basis of chemically related compounds.[12]

We proposed a computational protocol to obtain the reduction potential in which the electronic energies of the involved species are treated at the TPSSh/def2-QZVP level of theory and the solvation energies are obtained through the SMD model, with electrostatic interactions computed with the COSMO model. The method was calibrated with reactions involving NOx species, and the results are in good agreement with the experimental measurements. We also have shown that, for the reduction processes involving proton transfer, treating the proton as a Zundel cation significantly improves the results.

Combining with our previous *ab initio* molecular dynamics simulation of NO in aqueous solution, we proposed two pathways for the production of HNO through reduction of NO. The first pathway is the direct reduction of NO through proton-coupled electron transfer to produce HNO and the second path is the reduction of the radical anion $HONO^{\bullet-}$, which is involved in equilibrium with NO in aqueous solution. We have shown that both pathways are viable processes under physiological conditions, having reduction potentials of $E^{\circ\prime} = -0.161$ V and $E^{\circ\prime} \approx 1$ V for the first and second pathways, respectively. The results show that both processes can be promoted by well-known biological reductants such as NADH, vitamin C, vitamin E, cysteine, and glutathione, for which the reduction potential is around -0.3 to -0.5 V. In addition, the computed reduction potential of NO through the radical anion $HONO^{\bullet-}$ can explain the recent experimental findings on the formation of HNO through the reduction of NO, promoted by H_2S,[49−52] vitamin C, and aromatic alcohols.[14,15] Therefore, we believe that results presented in this work may contribute significantly to shed some light onto the question of whether and how HNO is produced in vivo and also for the understanding of the biochemical and physiological effects of NO.

ASSOCIATED CONTENT

Supporting Information

The Supporting Information is available free of charge on the ACS Publications website at DOI: 10.1021/acs.jpcb.7b03552.

Figure showing the gas phase TPSSh/Def2-QZVP optimized structures used to compute the reduction potential of all species quoted in Table 3 of the manuscript and table showing Cartesian coordinates of the gas phase TPSSh/Def2-QZVP optimized structures used to compute the reduction potential of all species quoted in Table 3 of the manuscript (PDF)

AUTHOR INFORMATION

Corresponding Authors

*E-mail: doctorovich@qi.fcen.uba.ar.
*E-mail: wrocha@ufmg.br.

ORCID

Willian R. Rocha: 0000-0002-0025-2158

Notes

The authors declare no competing financial interest.

ACKNOWLEDGMENTS

The authors would like to thank the CNPq (Conselho Nacional de Desenvolvimento Científico e Tecnológico, INCT-Catálise) and FAPEMIG (Fundação de Amparo à Pesquisa do Estado de Minas Gerais) and ANPCYT (PICT 2014-1278) for the financial support and research grants. F.D. is a member of CONICET.

REFERENCES

(1) Ignarro, L. J.; Buga, G. M.; Wood, K. S.; Byrnes, R. E.; Chaudhuri, G. Endothelium-derived Relaxing Factor Produced and Released from Artery and Vein is Nitric Oxide. *Proc. Natl. Acad. Sci. U. S. A.* **1987**, *84*, 9265−9269.

(2) Palmer, R. M. J.; Ashton, D. S.; Moncada, S. Vascular Endothelial Cells Synthesize Nitric Oxide from L-arginine. *Nature* **1988**, *333*, 664−666.

(3) Ignarro, L. J.; Murad, F. *Nitric Oxide: Biochemistry, Molecular Biology and Therapeutic Implications*; Academic Press: San Diego, CA, 1995.

(4) Ignarro, L. J. Endothelium-Derived Nitric Oxide: Pharmacology and Relationship to the Actions of Organic Nitrate Esters. *Pharm. Res.* **1989**, *6*, 651−659.

(5) Culotta, E.; Koshland, D. E. NO News is Good news. *Science* **1992**, *258*, 1862−1865.

(6) Feldman, P. L.; Griffith, O. W.; Stuehr, D. The Surprising Life of Nitric Oxide. *Chem. Eng. News* **1993**, *71*, 26−38.

DOI: 10.1021/acs.jpcb.7b03552
J. Phys. Chem. B 2017, 121, 6618−6625

(7) Richter-Addo, G. B.; Legzdins, P. *Metal Nitrosyls*; Oxford University Press: New York, 1992.
(8) Wink, A. A.; Darbyshire, J. F.; Nims, R. W.; Saavedra, J. E.; Ford, P. C. Reactions of the Bioregulatory Agent Nitric Oxide in Oxygenated Aqueous Media: Determination of the Kinetics for Oxidation and Nitrosation by Intermediates Generated in the NO/O_2 Reaction. *Chem. Res. Toxicol.* **1993**, *6*, 23−27.
(9) Chiang, T. M.; Sayre, R. M.; Dowdy, J. C.; Wilkin, N. K.; Rosenberg, E. W. Sunscreen ingredients inhibit inducible nitric oxide synthase (iNOS): a possible biochemical explanation for the sunscreen melanoma controversy. *Melanoma Res.* **2005**, *15*, 3−6.
(10) Weller, R. Nitric Oxide: A Key Mediator in Cutaneous Physiology. *Clin. Exp. Dermatol.* **2003**, *28*, 511−514.
(11) Stamler, J. S.; Singel, D. J.; Loscalzo, J. Biochemistry of nitric oxide and its redox-activated forms. *Science* **1992**, *258*, 1898−1902.
(12) Shafirovich, V.; Lymar, S. V. Nitroxyl and its Anion in Aqueous Solutions: Spin States, Protic Equilibria, and Reactivities Toward Oxygen and Nitric Oxide. *Proc. Natl. Acad. Sci. U. S. A.* **2002**, *99*, 7340−7345.
(13) Bartberger, M. D.; Liu, W.; Ford, E.; Miranda, K. M.; Switzer, C.; Fukuto, J. M.; Farmer, P. J.; Wink, D. A.; Houk, K. N. The Reduction Potential of Nitric Oxide (NO) and its Importance to NO Biochemistry. *Proc. Natl. Acad. Sci. U. S. A.* **2002**, *99*, 10958−10963.
(14) Hamer, M.; Suarez, S. A.; Neuman, N. I.; Alvarez, L.; Muñoz, M.; Marti, M. A.; Doctorovich, F. Discussing Endogenous NO•/HNO Interconversion Aided by Phenolic Drugs and Vitamins. *Inorg. Chem.* **2015**, *54*, 9342−9350.
(15) Suarez, A. A.; Neuman, N. I.; Muñoz, M.; Álvarez, L.; Bikiel, D. E.; Brondino, C. D.; Ivanović-Burmazović, I.; Miljkovic, J. L.; Filipovic, M. R.; Martí, M. A.; Doctorovich, F. Nitric Oxide Is Reduced to HNO by Proton-Coupled Nucleophilic Attack by Ascorbate, Tyrosine, and Other Alcohols. A New Route to HNO in Biological Media? *J. Am. Chem. Soc.* **2015**, *137*, 4720−4727.
(16) Zhang, Y. Computational Investigations of HNO in Biology. *J. Inorg. Biochem.* **2013**, *118*, 191−200.
(17) Parr, R. G.; Yang, W. *Density Functional Theory of Atoms and Molecules*; Oxford University Press: New York, 1989.
(18) Staroverov, V. N.; Scuseria, G. E.; Tao, J.; Perdew, J. P. Comparative assessment of a new nonempirical density functional: Molecules and hydrogen-bonded complexes. *J. Chem. Phys.* **2003**, *119*, 12129−12137.
(19) Shavitt, I.; Bartlett, R. J. *Many-Body Methods in Chemistry and Physics: MBPT and Coupled-Cluster Theory*; Cambridge University Press: New York, 2009.
(20) Neese, F.; Liakos, D. G.; Ye, S. F. Correlated Wavefunction Methods in Bioinorganic Chemistry. *JBIC, J. Biol. Inorg. Chem.* **2011**, *16*, 821−829.
(21) Harvey, J. N. The coupled-cluster description of electronic structure: perspectives for bioinorganic chemistry. *JBIC, J. Biol. Inorg. Chem.* **2011**, *16*, 831−839.
(22) Weigend, F.; Ahlrichs, R. Balanced basis sets of split valence, triple zeta valence and quadruple zeta valence quality for H to Rn: Design and assessment of accuracy. *Phys. Chem. Chem. Phys.* **2005**, *7*, 3297−3305.
(23) Marenich, A. V.; Cramer, C. J.; Truhlar, D. G. Universal solvation model based on solute electron density and on a continuum model of the solvent defined by the bulk dielectric constant and atomic surface tensions. *J. Phys. Chem. B* **2009**, *113*, 6378−6396.
(24) Klamt, A.; Schuurmann, G. COSMO: a new approach to dielectric screening in solvents with explicit expressions for the screening energy and its gradient. *J. Chem. Soc., Perkin Trans. 2* **1993**, 799−805.
(25) Allen, M. P.; Tildesley, D. J. *Computer Simulation of Liquids*; Oxford University Press: Oxford, U.K., 1989.
(26) Jorgensen, W. L.; Chandrasekhar, J.; Madura, J. D.; Impey, R. W.; Klein, M. L. Comparison of simple potential functions for simulating liquid water. *J. Chem. Phys.* **1983**, *79*, 926−935.
(27) Jorgensen, W. L.; Maxwell, D. S.; Tirado-Rives, J. Development and Testing of the OPLS All-Atom Force Field on Conformational Energetics and Properties of Organic Liquids. *J. Am. Chem. Soc.* **1996**, *118*, 11225−11236.
(28) Breneman, C. M.; Wiberg, K. B. Determining atom-centered monopoles from molecular electrostatic potentials. The need for high sampling density in formamide conformational analysis. *J. Comput. Chem.* **1990**, *11*, 361−373.
(29) Coutinho, K.; Canuto, S.; Zerner, M. C. A Monte Carlo-Quantum Mechanics study of the solvatochromic shifts of the lowest transition of benzene. *J. Chem. Phys.* **2000**, *112*, 9874−9880.
(30) Canuto, S.; Coutinho, K. From Hydrogen Bond to Bulk: Solvation Analysis of the $n\rightarrow\pi^*$ Transition of Formaldehyde in Water. *Int. J. Quantum Chem.* **2000**, *77*, 192−198.
(31) Coutinho, K.; Canuto, S. *DICE (Version 2.9): A Monte Carlo Program for Liquid Simulation*; University of São Paulo: São Paulo, Brazil, 2003.
(32) Åqvist, J.; Medina, C.; Samuelson, J.-E. A new method for predicting binding affinity in computer-aided drug design. *Protein Eng., Des. Sel.* **1994**, *7*, 385−391.
(33) Carlson, H. A.; Jorgensen, W. L. An Extended Linear Response Method for Determining Free Energies of Hydration. *J. Phys. Chem.* **1995**, *99*, 10667−10673.
(34) De Lima, G. F.; Duarte, H. A.; Pliego, J. R., Jr. Dynamical Discrete/Continuum Linear Response Shells Theory of Solvation: Convergence Test for NH_4^+ and OH^- Ions in Water Solution Using DFT and DFTB Methods. *J. Phys. Chem. B* **2010**, *114*, 15941−15947.
(35) Neese, F. The ORCA program system. *Wiley Interdiscip. Rev.: Comput. Mol. Sci.* **2012**, *2*, 73−78.
(36) Rulíšek, L. On the Accuracy of Calculated Reduction Potentials of Selected Group 8 (Fe, Ru, and Os) Octahedral Complexes. *J. Phys. Chem. C* **2013**, *117*, 16871−16877.
(37) Isse, A. A.; Gennaro, A. Absolute Potential of the Standard Hydrogen Electrode and the Problem of Interconversion of Potentials in Different Solvents. *J. Phys. Chem. B* **2010**, *114*, 7894−7899.
(38) Rodrigues, G. L. S.; Rocha, W. R. Formation and Release of NO from Ruthenium Nitrosyl Ammine Complexes $[Ru(NH_3)_5(NO)]^{2+/3+}$ in aqueous solution: A Theoretical Investigation. *J. Phys. Chem. B* **2016**, *120*, 11821−11833.
(39) Venâncio, M. F.; Rocha, W. R. Ab initio molecular dynamics simulation of aqueous solution of nitric oxide in different formal oxidation states. *Chem. Phys. Lett.* **2015**, *638*, 9−14.
(40) Stanbury, D. M. Reduction Potentials Involving Inorganic Free Radicals in Aqueous Solution. *Adv. Inorg. Chem.* **1989**, *33*, 69−138.
(41) Anderson, W. R. Heats of formation of HNO and some related species. *Combust. Flame* **1999**, *117*, 394−403.
(42) Chase, M. W., Jr. *J. Phys. Chem. Ref. Data*, Monograph 9 (Part I and Part II), 1998.
(43) Bratsch, S. G. Standard electrode potentials and temperature coefficients in water at 298.15 K. *J. Phys. Chem. Ref. Data* **1989**, *18*, 1−21.
(44) Dutton, A. S.; Fukuto, J. M.; Houk, K. N. Theoretical reduction potentials for nitrogen oxides from CBS-QB3 energetics and (C)PCM solvation calculations. *Inorg. Chem.* **2005**, *44*, 4024−4028.
(45) Kirchner, B. Eigen or Zundel ion: news from calculated and experimental photoelectron spectroscopy. *ChemPhysChem* **2007**, *8*, 41−43.
(46) Powell, D. R.; Adams, E. T., Jr. Self-association of gases 1. Theory. Application to the nitrogen dioxide-dinitrogen tetraoxide system. *J. Phys. Chem.* **1978**, *82*, 1947−1952.
(47) Haynes, W. M. *CRC Handbook of Chemistry and Physics*, 92th ed.; CRC Press: Boca Raton, FL, 2011.
(48) *MarvinView* (version 17.4.30), 2017, ChemAxon (http://www.chemaxon.com), accessed June 16, 2017.
(49) Eberhardt, M.; Dux, M.; Namer, B.; Miljkovic, J.; Cordasic, N.; Will, C.; Kichck, T. I.; De la Roche, J.; Fischer, M.; Suárez, S. A.; Bikiel, D.; Dorsch, K.; Leffler, A.; Babes, A.; Lampert, A.; Lennerz, J. K.; Johannes, J.; Martí, M. A.; Doctorovich, F.; Högestätt, E. D.; Zygmunt, P. M.; Ivanovic-Burmazovic, I.; Messlinger, K.; Reeh, P.; Filipovic, M. R. H_2S and NO cooperatively regulate vascular tone by activating a

DOI: 10.1021/acs.jpcb.7b03552
J. Phys. Chem. B 2017, 121, 6618−6625

neuroendocrine HNO−TRPA1−CGRP signalling pathway. *Nat. Commun.* **2014**, *5*, 4381−4397.
(50) Filipovic, M. R.; Eberhardt, M.; Prokopovic, V.; Mijuskovic, A.; Orescanin-Dusic, Z.; Reeh, P.; Ivanovic-Burmazovic, I. Beyond H2S and NO interplay: hydrogen sulfide and nitroprusside react directly to give nitroxyl (HNO). A new pharmacological source of HNO. *J. Med. Chem.* **2013**, *56*, 1499−1508.
(51) Filipovic, M. R. M.; Miljkovic, J. L. J.; Nauser, T.; Royzen, M.; Klos, K.; Shubina, T.; Koppenol, W. H.; Lippard, S. J.; Ivanović-Burmazović, I.; Ivanovic, I. Chemical Characterization of the Smallest S-Nitrosothiol, HSNO; Cellular Cross-talk of H_2S and S-Nitrosothiols. *J. Am. Chem. Soc.* **2012**, *134*, 12016−12027.
(52) Miljkovic, J. L.; Kenkel, I.; Ivanović-Burmazović, I.; Filipovic, M. R. Generation of HNO and HSNO from Nitrite by Heme-Iron-Catalyzed Metabolism with H_2S. *Angew. Chem., Int. Ed.* **2013**, *52*, 12061−12064.
(53) Harvey, J. N. Understanding the Kinetics of Spin-Forbidden Chemical Reactions. *Phys. Chem. Chem. Phys.* **2007**, *9*, 331−343.
(54) Lykhin, A. O.; Kaliakin, D. S.; dePolo, G. E.; Kuzubov, A. A.; Varganov, S. A. Nonadiabatic Transition State Theory: Application to Intersystem Crossings in the Active Sites of Metal-Sulfur Proteins. *Int. J. Quantum Chem.* **2016**, *116*, 750−761.

DOI: 10.1021/acs.jpcb.7b03552
J. Phys. Chem. B 2017, 121, 6618−6625